MITF links differentiation with cell cycle arrest in melanocytes by transcriptional activation of INK4A

Amy E. Loercher, Elizabeth M.H. Tank, Rachel B. Delston, and J. William Harbour

Department of Ophthalmology and Visual Sciences, Washington University School of Medicine, St. Louis, MO 63110

Cell cycle exit is required for proper differentiation in most cells and is critical for normal development, tissue homeostasis, and tumor suppression. However, the mechanisms that link cell cycle exit with differentiation remain poorly understood. Here, we show that the master melanocyte differentiation factor, microphthalmia transcription factor (MITF), regulates cell cycle exit by activating the cell cycle inhibitor INK4A, a tumor suppressor that frequently is mutated in melanomas. MITF binds the INK4A promoter, activates $p16^{Ink4a}$ mRNA and protein expression, and induces retinoblastoma protein hypophosphorylation, thereby triggering cell cycle arrest. This activation of INK4A was required for efficient melanocyte differentiation. Interestingly, MITF was also required for maintaining INK4A expression in mature melanocytes, creating a selective pressure to escape growth inhibition by inactivating INK4A. These findings demonstrate that INK4A can be regulated by a differentiation factor, establish a mechanistic link between melanocyte differentiation and cell cycle exit, and potentially explain the tissue-specific tendency for INK4A mutations to occur in melanoma.

Introduction

Terminal differentiation is accompanied by cell cycle exit in most cell types, and this proclivity for mature cells to stop dividing is important for normal development, tissue homeostasis, and tumor suppression (Lipinski and Jacks, 1999). In fact, the normal cellular function of many tumor suppressors is to regulate differentiation and cell cycle exit (Lipinski and Jacks, 1999). Nevertheless, the mechanisms that link differentiation with cell cycle exit remain poorly understood.

Melanocytes are derived from neural crest and differentiate under the control of microphthalmia transcription factor (MITF), a basic helix-loop-helix leucine zipper transcription factor that activates genes involved in pigment production (e.g., DCT, TYR, and TRP1) and melanocyte survival (e.g., BCL2) (McGill et al., 2002; Bear et al., 2003; Widlund and Fisher, 2003). Whether MITF also regulates cell cycle exit and maintenance of the post-mitotic state in melanocytes is unclear. We address that question here by investigating how MITF affects the Rb-$p16^{Ink4a}$ pathway, which plays a key role in cell cycle exit and orderly progression through the differentiation process in many cell types (Lipinski and Jacks, 1999).

The online version of this article includes supplemental material.

Correspondence to J. William Harbour: harbour@wustl.edu

Abbreviations used in this paper: MEF, mouse embryonic fibroblast; MITF, microphthalmia transcription factor; Rb, retinoblastoma protein; siRNA, small interfering RNA.

Results and discussion

To examine the role of MITF in melanocyte cell cycle regulation, we studied embryonic fibroblasts that differentiate into melanocytes under the influence of ectopic MITF, as previously characterized (Tachibana et al., 1996; Bear et al., 2003). Expression of MITF in 10T1/2 cells, which produce negligible endogenous MITF protein (Fig. 1 A), resulted in marked growth inhibition and morphologic changes consistent with melanocyte differentiation (Fig. 1 B). BrdU incorporation assays indicated that this growth block was due to cell cycle arrest (Fig. 1 C). In contrast, no cell cycle alterations were observed in cells expressing a MITF mutant lacking DNA-binding activity (MITF-DB; Fig. 1 C), indicating that the ability of MITF to negatively regulate the cell cycle is dependent on its DNA-binding activity.

Consequently, we reasoned that the cell cycle inhibitory activity of MITF might be mediated through interaction of the MITF DNA-binding domain with cell cycle gene promoter elements. The canonical MITF recognition motif consists of a distal M box containing a consensus CATGTG near the center and a proximal E box (CANNTG) (Yasumoto et al., 1995). A search of cell cycle regulatory gene promoters revealed multiple M and E boxes in the promoter region of INK4A in both human and mouse (Fig. 2 A). This finding was particularly interesting because INK4A is a tumor suppressor that is frequently inactivated in melanoma (Chin et al., 1998). Using chromatin immunoprecipitation assays, endogenous MITF from normal

The Journal of Cell Biology, Vol. 168, No. 1, January 3, 2005 35–40
http://www.jcb.org/cgi/doi/10.1083/jcb.200410115

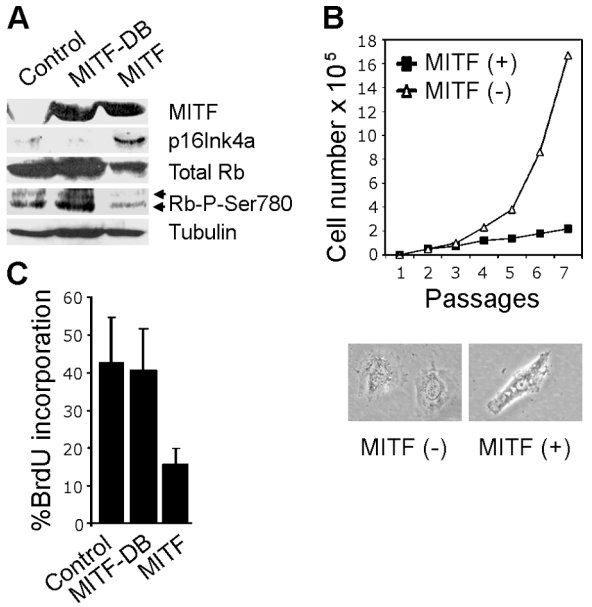

Figure 1. **MITF inhibits cell proliferation.** (A) Western blot demonstrating MITF, $p16^{Ink4a}$, total Rb, Rb-phospho-Ser780, and tubulin protein expression in 10T1/2 mouse fibroblasts stably expressing ectopic MITF, MITF-DB (DNA-binding mutant), or empty control vector. Arrows indicate hyperphosphorylated (top band) and hypophosphorylated (bottom band) forms of Rb. (B) Growth curves of 10T1/2 cells stably expressing MITF or empty control vector. Panels show morphology of 10T1/2 cells expressing control empty vector (left) and MITF (right). (C) BrdU incorporation assays in 10T1/2 cells expressing ectopic MITF , MITF-DB, or empty control vector.

melanocytes was detected at the INK4A promoter in vivo (Fig. 2 B). Consistent with this finding, gel mobility shift assays showed binding of endogenous MITF from Mel202 melanoma cells to M and E box elements from the INK4A promoter in vitro (Fig. S1, available at http://www.jcb.org/cgi/content/full/jcb.200410115/DC1). Competition with either the unlabeled M box or the unlabeled E box oligonucleotide inhibited binding of the other labeled oligonucleotides, suggesting that both elements are required for maximal binding of MITF to the INK4A promoter.

The ability of MITF to activate the INK4A promoter was tested using an INK4A promoter driving a luciferase reporter in 10T1/2 cells. Expression of MITF in these cells caused a dose-dependent increase in luciferase activity, with up to 20-fold induction compared with cells transfected with MITF-DB expression plasmid or a control empty vector (Fig. 2 C). In contrast, no induction was seen when two nucleotides in the M box sequence were mutated, indicating that activation of the INK4A promoter by MITF requires the MITF-binding motif. Consistent with these results, ectopic expression of MITF (but not MITF-DB) resulted in a substantial increase in endogenous $p16^{Ink4a}$ protein and mRNA levels in 10T1/2 cells (Fig. 1 A and Fig. 3 A).

Because $p16^{Ink4a}$ induces a G1 cell cycle arrest by inhibiting Cdk4 and allowing the accumulation of hypophosphorylated retinoblastoma protein (Rb) (Serrano et al., 1993), we examined the Rb protein in 10T1/2 cells after ectopic expression

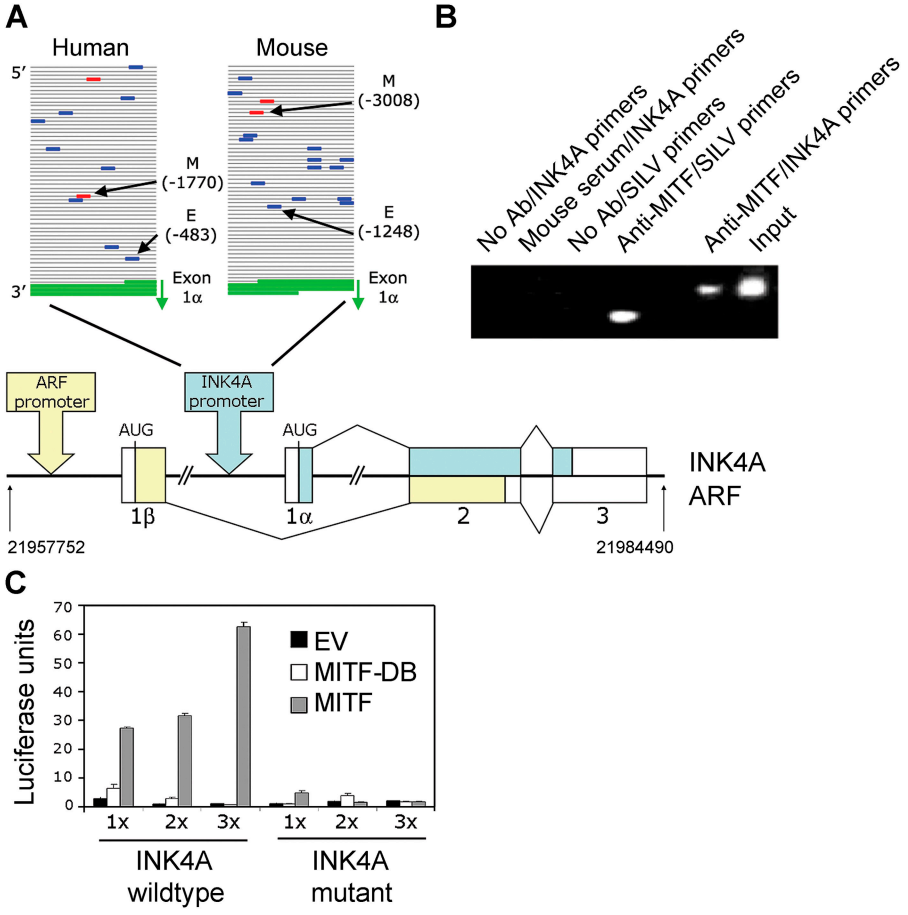

Figure 2. **MITF activates the INK4A gene.** (A) The ARF/INK4A locus (also called CDKN2A) and location of MITF-binding sites in the INK4A promoter. Exons 1α, 1β, 2, and 3 are indicated, along with their contribution to the INK4A and ARF mRNA transcripts. The nucleotide positions, relative to the centromere, are indicated. The INK4A promoter region is located upstream of exon 1α and downstream of exon 1β, which is transcribed only in the p14ARF transcript. A distinct ARF promoter is located upstream of exon 1β. Above the locus map, the INK4A promoter is depicted in greater detail for both human and mouse. Each line represents 70 bases of FASTA sequence from the NCBI web site (http://www.ncbi.nlm.nih.gov). Blue bars represent E boxes and red bars M boxes. The E box and M box nearest to the start site in exon 1α (green lines) are indicated. The direction of transcription is indicated by green arrows. (B) Chromatin immunoprecipitation assay in normal melanocytes. Chromatin was immunoprecipitated with an anti-MITF antibody or control mouse IgG, and then was PCR amplified using primers for the INK4A promoter or the SILV gene promoter, a known MITF target. (C) Luciferase assays in 10T1/2 cells transfected with expression vectors for MITF, MITF-DB, or an empty vector control (EV), along with a luciferase reporter driven by the INK4A promoter or a mutant INK4A promoter containing two nucleotide substitutions in the M box (1x, 2x, and 3x = 1-, 2-, and 3-μg plasmid DNA, respectively).

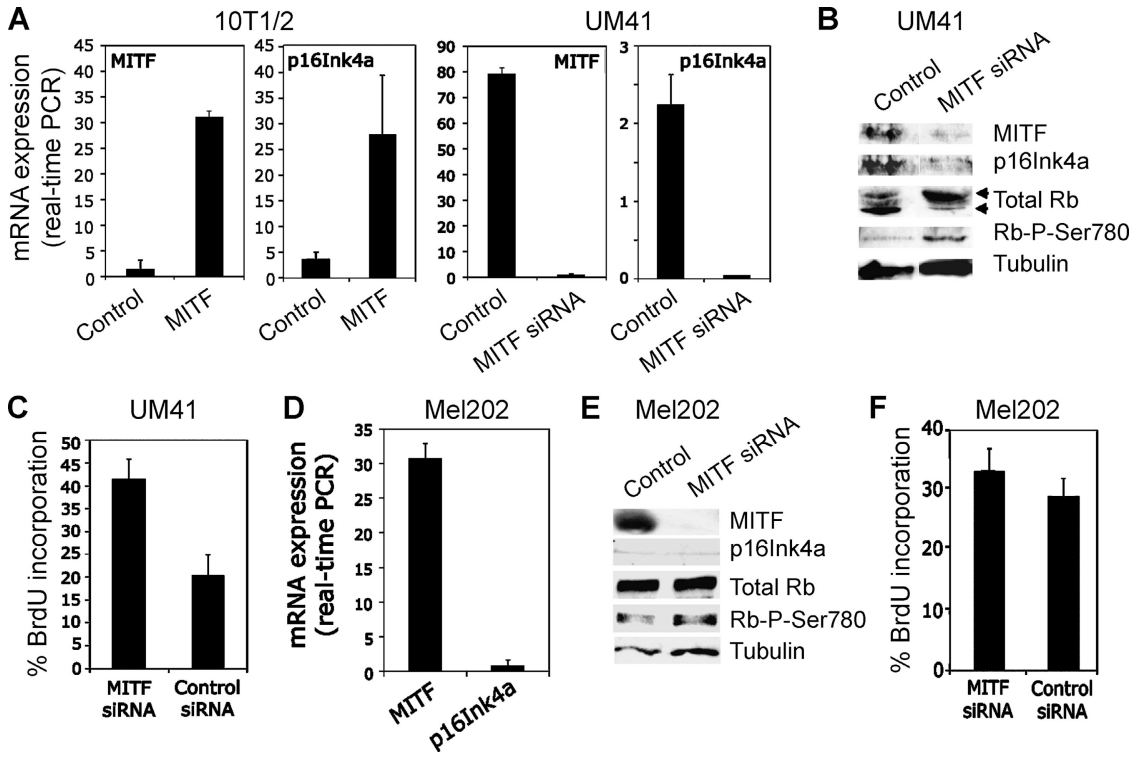

Figure 3. **MITF regulates p16^{Ink4a} and Rb in normal melanocytes, but not in melanoma cells.** (A) Real-time PCR assays of MITF and INK4A mRNA levels in 10T1/2 cells expressing ectopic MITF or an empty control vector (left panels) and in UM41 normal melanocytes transfected with MITF siRNA or control scrambled siRNA (right panels). Expression values represent fold difference compared with GAPDH. (B) Western blot analysis of MITF, p16^{Ink4a}, total Rb, Rb-phospho-Ser780, and tubulin protein expression in UM41 cells 48 h after transfection with plasmids expressing MITF siRNA or control scrambled siRNA. Arrows indicate hyperphosphorylated (top band) and hypophosphorylated (bottom band) forms of Rb. (C) BrdU incorporation assays in UM41 cells transfected with MITF siRNA or control scrambled siRNA. (D) Real-time PCR assays of MITF and p16^{Ink4a} mRNA levels in untransfected Mel202 melanoma cells. (E) Western blot analysis of MITF, p16^{Ink4a}, total Rb, Rb-phospho-Ser780, and tubulin protein expression in Mel202 cells 48 h after transfection with plasmids expressing MITF siRNA or control scrambled siRNA. (F) BrdU incorporation assay in Mel202 cells expressing MITF siRNA or control scrambled siRNA.

of MITF or MITF-DB. Neither MITF nor MITF-DB affected total Rb protein levels in 10T1/2 cells, but only MITF induced an accumulation of hypophosphorylated Rb (Fig. 1 A). In particular, MITF expression resulted in loss of phosphorylation at Ser780, a CDK site that is preferentially phosphorylated by the p16^{Ink4a} target Cdk4 and is known to be involved in regulation of cell division and differentiation (Kitagawa et al., 1996; Brugarolas et al., 1999; Ma et al., 2003).

To investigate whether MITF is required to sustain endogenous p16^{Ink4a} expression in melanocytic cells, we depleted MITF in early passage normal melanocytes by RNA interference. Compared with melanocytes transfected with control scrambled small interfering RNA (siRNA) expression vector, those transfected with MITF siRNA expression vector exhibited markedly reduced levels of MITF and p16^{Ink4a} mRNA and protein (Fig. 3, A and B). These changes were accompanied by an accumulation of hyperphosphorylated Rb (Fig. 3 B). Consistent with these findings, depletion of MITF caused melanocytes to reenter the cell cycle, as evidenced by increased BrdU incorporation (Fig. 3 C), suggesting that the MITF-p16^{Ink4a}-Rb pathway is also important for maintenance of the post-mitotic state in mature melanocytes. In contrast to normal melanocytes, depletion of MITF in Mel202 melanoma cells, which express low levels of p16^{Ink4a} (Fig. 3 D) as a result of promoter methylation (van der Velden et al., 2001), had no effect on p16^{Ink4a} or Rb protein levels, Rb phosphorylation, or BrdU incorporation (Fig. 3, E and F). Thus, MITF induces and maintains cell cycle exit in melanocytes, but this regulatory mechanism can be disrupted in melanoma cells by inactivation of INK4A.

Next, we established colonies of 10T1/2 cells stably expressing MITF and passaged them every 3 d, monitoring for changes in growth rate. As described above, cells expressing MITF initially exhibited a dramatically reduced growth rate. However, after four or more passages occasional clones escaped the MITF-induced inhibition and began growing at a rate comparable to parental cells that did not express MITF (Fig. 4 A). In these escape clones, MITF mRNA and protein levels remained unchanged, but p16^{Ink4a} mRNA and protein were markedly reduced (Fig. 4, B and C). Further, methylation-specific PCR assays revealed methylation of CpG islands (indicative of gene inactivation) within the INK4A promoter in the escape clones, but not in the growth-inhibited clones (Fig. 4 D). The level of methylation was similar to that observed in Mel202 melanoma cells. Thus, inactivation of INK4A provides an escape from MITF-induced growth inhibition, which may explain the strong selective pressure to silence INK4A during melanoma formation (Chin et al., 1998).

Next, we examined whether melanocyte differentiation and cell cycle arrest are independent processes. MITF and

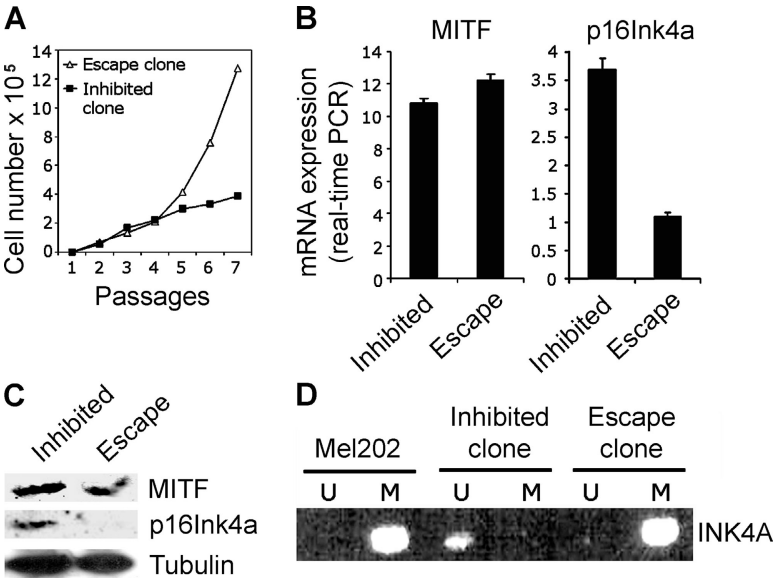

Figure 4. **Cells that escape MITF-induced growth inhibition exhibit silencing of INK4A.** (A) Growth curve of 10T1/2 cells stably expressing ectopic MITF. Growth-inhibited and escape clones are indicated. (B) Real-time PCR measurement of MITF and $p16^{Ink4a}$ mRNA levels in a growth-inhibited clone and an escape clone. Expression values are fold difference compared with GAPDH. (C) Western blot analysis of MITF, $p16^{Ink4a}$, and tubulin protein expression in a growth-inhibited clone and an escape clone. (D) Methylation-specific PCR of CpG island in the INK4A promoter region in a growth-inhibited clone and an escape clone, as well as in Mel202 cells. "U" indicates unmethylated and "M" indicates methylated primer sets.

MITF-DB were expressed in wild-type and INK4A-null primary mouse embryonic fibroblasts (MEFs), and then were monitored for growth rate and morphology. As expected, MITF (but not MITF-DB) inhibited the growth of wild-type cells, but it had no growth inhibitory effect on INK4A-null cells (Fig. 5 A). MITF efficiently blocked cell cycle progression in wild-type cells as measured by BrdU incorporation, whereas no cell cycle inhibition was observed in INK4A-null cells (Fig. 5 B). As with the 10T1/2 cells, MEFs expressing ectopic MITF exhibited morphologic changes consistent with melanocyte differentiation (Fig. 5 C), but MITF did not induce these changes in cells lacking INK4A (Fig. 5 C). Likewise, the melanocyte differentiation marker S100 was detected in MITF-expressing cells that were wild type for INK4A but not in those that were null for INK4A (Fig. 5 D). Importantly, ectopic MITF and MITF-DB levels were similar in wild-type and INK4A-null MEFs (Fig. S2, available at http://www.jcb.org/cgi/content/full/jcb.200410115/DC1). These results suggest that MITF requires INK4A not only for cell cycle inhibition, but also for efficient execution of the melanocyte differentiation program. Indeed, Sviderskaya and coworkers found that melanocytes lacking INK4A were more proliferative and less differentiated than melanocytes having one or both copies of INK4A (Sviderskaya et al., 2002).

These findings provide new mechanistic insights into several biological problems. First, they provide an example of how differentiation can be linked with cell cycle arrest. By activating genes involved in cell cycle exit (i.e., INK4A) as

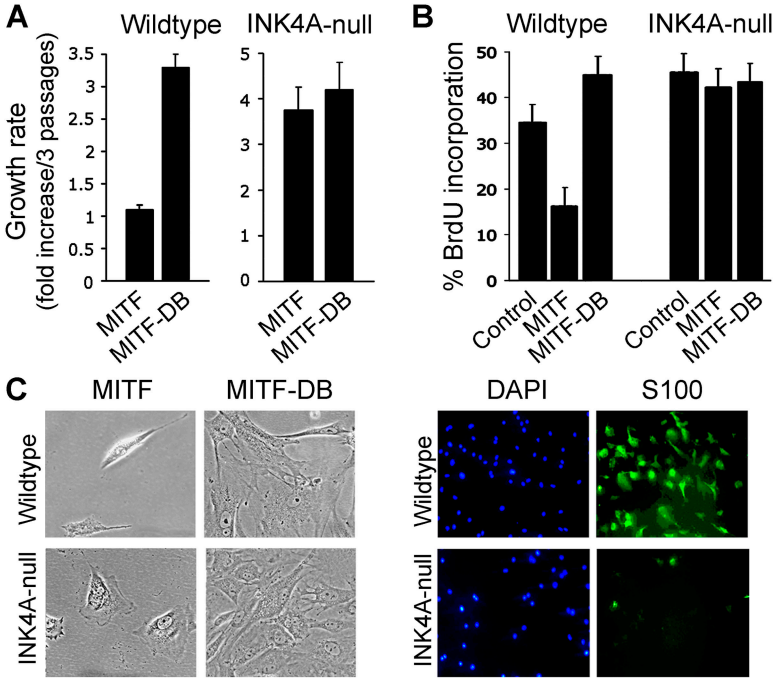

Figure 5 **INK4A is required for MITF to execute the melanocyte differentiation program.** (A) Growth rate of INK4A-wildtype and INK4A-null MEFs expressing ectopic MITF or MITF-DB. (B) BrdU incorporation assays in INK4A-wildtype and INK4A-null MEFs expressing ectopic MITF, MITF-DB, or empty control vector. (C) Phase-contrast photomicrographs (left panels) of INK4A-wildtype and INK4A-null MEFs expressing ectopic MITF or MITF-DB. Only MITF-expressing wild-type cells exhibit spindle morphology consistent with melanocyte differentiation. Immunofluorescence analysis (right panels) of INK4A-wildtype and INK4A-null MEFs expressing ectopic MITF. DAPI staining (blue) indicates cell nuclei, and green staining indicates expression of the melanocyte marker S100.

well as melanocyte cell fate, MITF efficiently coregulates these interrelated processes. Analogous to MITF, MyoD is a helix-loop-helix transcription factor that induces both cell cycle exit and differentiation in myoblasts (Sorrentino et al., 1990). However, unlike our findings for MITF, MyoD-induced cell cycle arrest does not appear to be a prerequisite for myoblast differentiation. Second, our results show that INK4A can be regulated directly by a differentiation factor. This is a particularly relevant point because surprisingly little is known about the transcriptional control of this important cell cycle regulator. Third, our results provide new insights into one of the most perplexing questions in cancer biology (Sherr, 2004): why are specific tumor suppressors (many of which are differentiation factors) associated with cancer in certain cell types but not others? Our findings would suggest that at least part of the answer lies in the mechanisms linking differentiation and cell cycle exit in a given cell type. The direct link between MITF and INK4A provides an attractive explanation for the strong association between INK4A mutation and melanoma (Ranade et al., 1995; Monzon et al., 1998). Why do melanocytes mutate INK4A rather than MITF or Rb? One potential explanation is that both MITF and Rb are required for melanocyte survival (Yavuzer et al., 1995; McGill et al., 2002; Yu et al., 2003), whereas INK4A appears only to regulate cell cycle.

A critical question that remains unanswered is how differentiation is prohibited in the absence of cell cycle exit. One speculation, based on the observation that E2F1 becomes bound to hypophosphorylated Rb during differentiation (Ikeda et al., 1996; Kastner et al., 1998), is that free E2F inhibits the differentiation program. Rb-E2F may then serve as a checkpoint to allow differentiation only when Rb is hypophosphorylated and able to induce G1 arrest. Further work is underway to address this question.

Materials and methods

Cells and transfection

Mel202 human melanoma cells were a gift of B. Ksander (Harvard, Boston, MA). C3H 10T1/2 and primary MEFs were obtained from American Type Culture Collection. Normal human melanocytes were described previously (Harbour et al., 2002). INK4A-null MEFs were generated at E13.5 from FVB.129-CDKN2atm2.1Rdp mice (from Mouse Models of Human Cancers Consortium, Frederick, MD). Cells were maintained in DME with 10% FCS. MITF expression vector in pT7T3D-PacI was obtained from American Type Culture Collection. MITF-DB was generated by introducing a T-to-A nucleotide substitution in the MITF DNA-binding domain using site-directed mutagenesis with QuickChange II (Stratagene), resulting in an *I*212*N* substitution, which inhibits DNA binding (Takebayashi et al., 1996). RNA interference was achieved using pSilencer plasmid (Ambion) expressing MITF siRNA or scrambled control siRNA (Xeragon). Luciferase assays were performed as described previously (Ma et al., 2003) using INK4A promoter-luciferase reporter (a gift of G. Gores, Mayo Medical School, Rochester, MN) or a mutant promoter generated by mutation of two nucleotides in the M box (CAACTG) using site-directed mutagenesis. Constructs were verified by sequencing. Transfections were performed with 1 μg test plasmid DNA (unless otherwise indicated) using Effectene (QIAGEN).

BrdU and immunofluorescence assays

BrdU and immunofluorescence assays were performed as described previously (Ma et al., 2003). In brief, 10^5 cells were transfected with the indicated expression vectors, along with a GFP vector (10:1 ratio), on coverslips. For BrdU assays, cells were labeled with BrdU (1:1,000 dilution; Amersham Biosciences) 24–72 h after transfection. After a further 12–36 h, cells were rinsed with 1× PBS, fixed in 3.7% formaldehyde for 15 min, permeabilized in 0.3% Triton X-100 for 15 min, and probed with an anti-BrdU antibody (BD Biosciences) at 1:200 dilution in immunofluorescence buffer for 1 h at 37°C in a humidified chamber. After washing the coverslips twice with 1 ml/well PBS, the cells were incubated with Alexa Fluor–conjugated secondary antibody (Molecular Probes, Inc.) at 1:1,000 dilution for 1 h. Cells were stained with DAPI, mounted onto slides using Vectashield mounting medium (Vector Laboratories) and analyzed by fluorescence microscopy. The percentage of cells incorporating BrdU was calculated from the fraction of GFP-positive transfected cells that were positive for BrdU staining. For other immunofluorescence assays, cells were incubated with anti-S100, anti-DCT, or anti-TRP1 primary antibodies and FITC- or Texas red–conjugated secondary antibodies (all from Santa Cruz Biotechnology, Inc.) and analyzed by fluorescence microscopy in a similar fashion.

Image acquisition

Microscopy was performed with an Olympus BX40 microscope (brightfield) and an Olympus BH-2 microscope (fluorescence) using an Olympus UPlanFL 40× magnification objective lens with 0.75 aperture. Photomicrographs were obtained at RT under air using the Olympus DP70 camera (brightfield) and the Insight Spot RT camera (fluorescence). The fluorochrome was Oregon green 488 (Molecular Probes, Inc.). Image acquisition was achieved with Olympus DP controller software. Minimal image processing was performed with Adobe Photoshop.

Western blot

Western blots were performed as described previously (Ma et al., 2003) using antibodies that recognize MITF (Oncogene Research Products), Rb (sc102; Santa Cruz Biotechnology, Inc.), Rb-phospho-Ser780 (Cell Signaling), $p16^{Ink4a}$ (Cell Signaling), and gamma-tubulin (Sigma-Aldrich).

Quantitative PCR

Total RNA was collected using TRIzol (Invitrogen), cDNA was generated using Superscript First Strand Synthesis (Invitrogen), and amplification was performed using the Platinum Quantitative PCR SuperMix-UDG kit (Invitrogen) according to manufacturer's instructions in an iCycler (Bio-Rad Laboratories). LUX Fluorogenic primers for MITF-M and INK4A transcripts were: MITF-forward 5′-CCGTTGGGCTTGCTGCATGT-3′, MITF-reverse 5′-CACCAACTACCGTCTCTACTGGATGG-3′, INK4A forward 5′-CGGTCCCCTCCAGAGGATTTG-3′, INK4A-reverse 5′-CACCGCTCCTCTTTCTTCCTCCGG-3′.

Methylation-specific PCR

Genomic DNA was isolated using the DNeasy Tissue kit (QIAGEN), was bisulfite modified, and was amplified with methylation-specific primers for INK4A promoter CpG islands. Primer sequences are as follows: methylated-forward 5′-TTTAAATACGTTTTTGTTGGTAGGC-3′, methylated-reverse 5′-ACGAATATAACACCCCTAAAATCG-3′, unmethylated-forward 5′-TAAATATGTTTTTGTTGGTAGGTGG-3′, and unmethylated-reverse 5′-CAAATATAACACCCCTAAAATCACC-3′. PCR was performed using 0.5 μg template, 20 pmol each primer, 1.25 mM dNTP, 6.75 mM $MgCl_2$, 10× PCR buffer (Invitrogen), and Taq Polymerase (Invitrogen). Reactions were run at 94°C for 5 min, followed by 35 cycles of 94°C (30 s), 53°C (30 s), and 72°C (30 s). PCR products were visualized on a 2.0% agarose gel containing ethidium bromide. Mel202 cells were used as a positive control.

Chromatin immunoprecipitation assays

ChIP assays were performed using a commercial kit (Upstate Biotechnology) as described by the manufacturer. In brief, 10^7 normal melanocytes were cross-linked in PBS containing proteinase inhibitors and 1% formaldehyde for 15 min at 37°C, scraped and centrifuged (4 min, 2,000 rpm, 4°C), resuspended in SDS lysis buffer with proteinase inhibitors, sonicated, and centrifuged (4 min, 2,000 rpm, RT). Dilution buffer was added, and supernatants were precleared with 75 μl salmon sperm DNA/protein A. 1 μl MITF antibody (Oncogene Research Products) or mouse IgG (negative control) was added overnight at 4°C, then 60 μl salmon sperm DNA/protein A was added for 1 h at 4°C. The slurry was pelleted (1 min, 1,000 rpm, 4°C), and was washed 5 min each with low salt wash, high salt wash, LiCl buffer, and TE buffer (10 mM Tris-HCl, pH 8.0, and 1 mM EDTA). Samples were treated with 250 μl elution buffer (1% SDS/0.1M $NaHCO_3$) at RT for 15 min, then with 20 μl of 5M NaCl at 65°C for 4 h, then with 0.5M EDTA/Tris-HCl and 2 μg proteinase K at 45°C for 1 h. DNA was purified using the DNEasy kit (QIAGEN). PCR to detect the INK4A and SILV promoters was performed with the following primers: INK4A-5′-AGCATGTGCCTGTAATCCCAGCTA-3′, INK4A-5′-TGGGAGA-

CAAGAGCGAAACTTGGT-3′, SILV-5′-CATGGAGAACTTCCAAAAGG-TGG-3′, and SILV-5′-TACTCTCCCCAGGGAGTATAAGT-3′.

Online supplemental material

Gel mobility shift assay demonstrates that MITF binds to the INK4A promoter elements, and that efficient binding requires both the E box and the M box (Fig. S1). Western blot analysis (Fig. S2 A) and immunofluorescence assays (Fig. S2 B) demonstrate that ectopic MITF is expressed at similar levels in wild-type and INK4A-null MEFs. Online supplemental material available at http://www.jcb.org/cgi/content/full/jcb.200410115/DC1.

We thank L. Worley for technical assistance.

This work was supported by grants from the National Institutes of Health (EY13169 to J.W. Harbour), Research to Prevent Blindness, Inc. (to J.W. Harbour), the Macula Society (to J.W. Harbour), and a National Institutes of Health training grant (T32 EY13360 to A.E. Loercher). Core grants from the National Eye Institute and Research to Prevent Blindness, Inc. to the Department of Ophthalmology and Visual Sciences were also used.

Submitted: 22 October 2004
Accepted: 17 November 2004

References

Bear, J., Y. Hong, and M. Schartl. 2003. Mitf expression is sufficient to direct differentiation of medaka blastula derived stem cells to melanocytes. *Development.* 130:6545–6553.

Brugarolas, J., K. Moberg, S.D. Boyd, Y. Taya, T. Jacks, and J.A. Lees. 1999. Inhibition of cyclin-dependent kinase 2 by p21 is necessary for retinoblastoma protein-mediated G1 arrest after gamma-irradiation. *Proc. Natl. Acad. Sci. USA.* 96:1002–1007.

Chin, L., G. Merlino, and R.A. DePinho. 1998. Malignant melanoma: modern black plague and genetic black box. *Genes Dev.* 12:3467–3481.

Harbour, J.W., L. Worley, D. Ma, and M. Cohen. 2002. Transducible peptide therapy for uveal melanoma and retinoblastoma. *Arch. Ophthalmol.* 120:1341–1346.

Ikeda, M.A., L. Jakoi, and J.R. Nevins. 1996. A unique role for the Rb protein in controlling E2F accumulation during cell growth and differentiation. *Proc. Natl. Acad. Sci. USA.* 93:3215–3220.

Kastner, A., X. Espanel, and G. Brun. 1998. Transient accumulation of retinoblastoma/E2F-1 protein complexes correlates with the onset of neuronal differentiation in the developing quail neural retina. *Cell Growth Differ.* 9:857–867.

Kitagawa, M., H. Higashi, H.K. Jung, T.I. Suzuki, M. Ikeda, K. Tamai, J. Kato, K. Segawa, E. Yoshida, S. Nishimura, and Y. Taya. 1996. The consensus motif for phosphorylation by cyclin D1-Cdk4 is different from that for phosphorylation by cyclin A/E-Cdk2. *EMBO J.* 15:7060–7069.

Lipinski, M.M., and T. Jacks. 1999. The retinoblastoma gene family in differentiation and development. *Oncogene.* 18:7873–7882.

Ma, D., P. Zhou, and J.W. Harbour. 2003. Distinct mechanisms for regulating the tumor suppressor and antiapoptotic functions of Rb. *J. Biol. Chem.* 278:19358–19366.

McGill, G.G., M. Horstmann, H.R. Widlund, J. Du, G. Motyckova, E.K. Nishimura, Y.L. Lin, S. Ramaswamy, W. Avery, H.F. Ding, et al. 2002. Bcl2 regulation by the melanocyte master regulator Mitf modulates lineage survival and melanoma cell viability. *Cell.* 109:707–718.

Monzon, J., L. Liu, H. Brill, A.M. Goldstein, M.A. Tucker, L. From, J. McLaughlin, D. Hogg, and N.J. Lassam. 1998. CDKN2A mutations in multiple primary melanomas. *N. Engl. J. Med.* 338:879–887.

Ranade, K., C.J. Hussussian, R.S. Sikorski, H.E. Varmus, A.M. Goldstein, M.A. Tucker, M. Serrano, G.J. Hannon, D. Beach, and N.C. Dracopoli. 1995. Mutations associated with familial melanoma impair $p16^{INK4}$ function. *Nat. Genet.* 10:114–116.

Serrano, M., G.J. Hannon, and D. Beach. 1993. A new regulatory motif in cell-cycle control causing specific inhibition of cyclin D/CDK4. *Nature.* 366:704–707.

Sherr, C.J. 2004. Principles of tumor suppression. *Cell.* 116:235–246.

Sorrentino, V., R. Pepperkok, R.L. Davis, W. Ansorge, and L. Philipson. 1990. Cell proliferation inhibited by MyoD1 independently of myogenic differentiation. *Nature.* 345:813–815.

Sviderskaya, E.V., S.P. Hill, T.J. Evans-Whipp, L. Chin, S.J. Orlow, D.J. Easty, S.C. Cheong, D. Beach, R.A. DePinho, and D.C. Bennett. 2002. $p16^{Ink4a}$ in melanocyte senescence and differentiation. *J. Natl. Cancer Inst.* 94:446–454.

Tachibana, M., K. Takeda, Y. Nobukuni, K. Urabe, J.E. Long, K.A. Meyers, S.A. Aaronson, and T. Miki. 1996. Ectopic expression of MITF, a gene for Waardenburg syndrome type 2, converts fibroblasts to cells with melanocyte characteristics. *Nat. Genet.* 14:50–54.

Takebayashi, K., K. Chida, I. Tsukamoto, E. Morii, H. Munakata, H. Arnheiter, T. Kuroki, Y. Kitamura, and S. Nomura. 1996. The recessive phenotype displayed by a dominant negative microphthalmia-associated transcription factor mutant is a result of impaired nucleation potential. *Mol. Cell. Biol.* 16:1203–1211.

van der Velden, P.A., J.A. Metzelaar-Blok, W. Bergman, H. Monique, H. Hurks, R.R. Frants, N.A. Gruis, and M.J. Jager. 2001. Promoter hypermethylation: a common cause of reduced $p16^{INK4a}$ expression in uveal melanoma. *Cancer Res.* 61:5303–5306.

Widlund, H.R., and D.E. Fisher. 2003. *Microphthalamia*-associated transcription factor: a critical regulator of pigment cell development and survival. *Oncogene.* 22:3035–3041.

Yasumoto, K., H. Mahalingam, H. Suzuki, M. Yoshizawa, and K. Yokoyama. 1995. Transcriptional activation of the melanocyte-specific genes by the human homolog of the mouse Microphthalmia protein. *J. Biochem. (Tokyo).* 118:874–881.

Yavuzer, U., E. Keenan, P. Lowings, J. Vachtenheim, G. Currie, and C.R. Goding. 1995. The Microphthalmia gene product interacts with the retinoblastoma protein in vitro and is a target for deregulation of melanocyte-specific transcription. *Oncogene.* 10:123–134.

Yu, B.D., M. Becker-Hapak, E.L. Snyder, M. Vooijs, C. Denicourt, and S.F. Dowdy. 2003. Distinct and nonoverlapping roles for pRB and cyclin D: cyclin-dependent kinases 4/6 activity in melanocyte survival. *Proc. Natl. Acad. Sci. USA.* 100:14881–14886.